J Math Chem (2013) 51:2120–2143
DOI 10.1007/s10910-013-0202-3

ORIGINAL PAPER

On modeling the dissolution of sedimentary rocks in acidic environments. An overview of selected mathematical methods with presentation of a case study

Cataldo De Blasio · Claudio Carletti · Tapio Westerlund · Mika Järvinen

Received: 2 March 2013 / Accepted: 27 May 2013 / Published online: 9 June 2013

Abstract Different environmental processes utilize calcium carbonate and sedimentary rocks, for instance sedimentary rocks are used for water purification as filters and utilized also for acid remediation of process waters before being discarded. Additionally sedimentary rocks are used in another very important environmental process, wet Flue Gas Desulfurization. In this process, limestone and carbonates in general play one important role because of their dissolution and provision of the necessary amount of calcium ions used for the precipitation of gypsum. The objective of this study is to present in a first place an overview of a reduced number of specific theoretical and empirical mathematical models applied to the dissolution of carbonates in acidic environments with provision of additional developments and details, secondly a case study was presented where a suitable time of exposure and surface diffusivity obtained analytically by different methods well describe the experimental results. There were justifications for this choice. The experimental data and the related mathematical modeling were performed considering transient conditions. In the present work diverse raw materials were tested in order to reveal their suitability for wet Flue Gas Desulfurization. The research was focused on products from CO_2 fixation processes materials as well as other types of limestone samples. In this way it was found that also waste materials from different environmental processes, like CO_2 fixation can be used for Flue Gas Desulfurization.

C. De Blasio (✉) · M. Järvinen
Laboratory of Energy Engineering and Environmental Protection, Department of Energy Technology, School of Engineering, Aalto University, Sähkömiehentie 4, Otaniemi, P.O. Box. 14400, Espoo, Finland
e-mail: cataldo.de.blasio@aalto.fi

C. Carletti · T. Westerlund
Faculty of Technology, Process Design and Systems Engineering, Åbo Akademi University, Biskopsgatan 8, 20500 Åbo, Finland

Keywords Gas Desulfurization · Limestone reactivity · Mathematical modeling · Transport phenomena

1 Introduction

The importance of Flue Gas Desulfurization, and CO_2 removal processes is well recognized because of the environmental and health problems caused by SO_2 and CO_2 compounds. Limestone and related calcium carbonate compounds are utilized widely for Wet Flue Gas Desulfurization, WFGD, and acid remediation of acidic process water. The reactivity of limestone and carbonates in liquids has been studied by several authors and with different experimental conditions. The preeminent method to test the reactivity of different qualities of materials is to utilize a system that simulates a slurry solution, the best way is to test the reactivity of the particles by means of diluted strong acids like hydrochloric acid [1,2]. Normally the particle size distribution (PSD) is taken into account and *pH* conditions are maintained at a constant level and at the same value utilized during the industrial process [3]. The correct evaluation of the Reynolds and Schmidt number allows us to evaluate the quality of the samples by estimating the time of exposure (TOE) [4,5]. The mathematical modeling of the transport phenomena and reaction rates involved is not always an easy task and the procedures can be quite articulate even for first order reaction kinetics [6]. Different experimental configurations are utilized; for instance the reactivity of limestone and dolomite in acidic environment have been modeled by rotating disks [7–9], particles in a packed bed reactor have been used to study the dissolution of dolomite in water at high temperatures [10]. Parallel plates are considered by B. Williams and collaborators [11], where different reaction kinetic models were taken into account. In the present study it was preferred to consider small particles free to move into the mixed slurry with turbulent conditions, this follows from reasoning on the effect the acid solution can have on the solid-liquid interface. Solid surfaces with cylindrical, spherical or disk shape have been mostly considered for studying heat transfer phenomena in liquid mediums [12], and considering the heat and mass transfer analogy, authors have started to use similar models for mass transfer phenomena; however there are some considerations to be done: we suppose that the solid surface of a fixed shape, for instance a disk, is in contact with a liquid for a short time; in this case it is reasonable to assume that dissolution does not change the solid surface, nevertheless not necessarily the composition of that surface is equal to the surface which immediately follows. For this reason statistical considerations suggest to use several surfaces or long reaction times. On the other end if we consider a long surface TOE, most likely the surface will be affected by the dissolution or reactions. The geological background and structure of carbonate rocks is also to be taken into consideration when the reactivity is modeled. The rate determining phenomena of the dissolution has being accounted as the mass-transfer of H^+ ions at low *pH* and as the surface reaction kinetics at higher values of *pH*. However, some controversy has been present in the literature regarding the borderline where surface reaction kinetics starts to prevail and also with respect to the kinetic order of the reaction [13]. Geological data of the particular samples were provided thanks to the collaboration with Tallin

University in Estonia and Åbo Akademi University in Finland, however the correlations between crystallographic structure, chemical compositions and reactivity need further investigation; this is because limestone rocks showing similar composition in fact have different reactivity.

2 Theory and overview of the mathematical models used

2.1 Main reactions involved in limestone-acid systems

Wet Flue Gas Desulfurization involves a three phase process which can be synthesized as follows [3,14]: the first step is the absorption of SO_2 (gas) into droplets of water in order to have SO_2 in a liquid phase. Here water is reacting with SO_2 and hydronium ions are then released; the forced convection of air is then applied to the tank reactor to allow for the oxidation steps shown in Table 1. Hydronium ions are formed from these reactions therefore an acidic environment is obtained in the reaction tank. Once the sulfate ions are formed, the dissolution of calcium carbonate compounds plays a key role in FGD because Ca^{++} ions produce gypsum from the reaction with sulfate and water. Gypsum is precipitated and collected at the end of the process. The reactions are presented in the following table.

Previous studies [1,9] have considered the reactivity of calcium carbonate in presence of strong acids like hydrochloric acid. In the following table the main reactions involved are given [1]:

Reaction shown in Table 2 are modeled as one single pseudo first order irreversible chemical reaction [15] as follows:

$$CaCO_3 + 2H^+ \rightarrow CO_2 + Ca^{2+} + H_2O \tag{1}$$

Equation (1) allows for important simplifications and it is confirmed when there is an acidic environment.

Table 1 The principal reactions taking place in wet FGD with forced oxidation

Rate determining steps	Reactions
Absorption of SO_2 in water	$SO_2 + H_2O \rightleftarrows H^+ + HSO_3^-$
	$HSO_3^- \rightleftarrows H^+ + SO_3^{2-}$
Oxidation of HSO_3^-	$HSO_3^- + \frac{1}{2}O_2 \rightleftarrows H^+ + SO_4^{2-}$
	$HSO_4^{2-} \rightleftarrows SO_4^{2-} + H^+$
Limestone dissolution	$CaCO_3 \rightleftarrows Ca^{2+} + CO_3^{2-}$
	$CO_2 + H_2O \rightleftarrows HCO_3^- + H^+$
	$HCO_3^- \rightleftarrows CO_3^{2-} + H^+$
	$H_2O \rightleftarrows H^+ + OH^-$
Crystallization of gypsum	$Ca^{2+} + SO_4^{2-} + 2H_2O \rightleftarrows CaSO_4 \cdot 2H_2O$

Table 2 Limestone dissolution in presence of hydronium ions

Fenomena	Reactions
Dissolution of limestone	$CaCO_3(s) \rightarrow Ca^{2+} + CO_3^{2-}$
Carbonate ions reacting with H^+	$H_3O^+ + CO_3^{2-} \rightarrow HCO_3^- + H_2O$
Carbonic ions with H^+	$HCO_3^- + H_3O^+ \rightarrow H_2CO_3 + H_2O$
Final products	$H_2CO_3 \rightarrow CO_2(g) + H_2O$

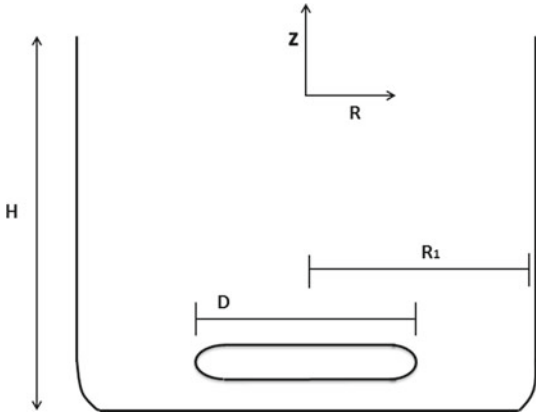

Fig. 1 BSTR system with main parameters

2.2 Importance of mixing

A simplified procedure for evaluating the quality of different kind of sedimentary rocks was tested taking into account the rate of mixing. The Reynolds and Schmidt numbers play an important role in modeling and evaluation of the necessary mixing rate necessary to suspend all the particles. The geometry to which we refer in order to evaluate the above mentioned value is described in Fig. 1.

The velocity along the angularity is $v_\theta = r * N$ where r is the generic radius and N is the frequency of the stirring. For this reason the Reynolds number for our system is [16]:

$$Re = \frac{d^2 N \rho}{\mu} \tag{2}$$

where ρ and μ are the density and the viscosity of the medium respectively. The Reynolds number represents the ratio of the inertial to viscous forces, we denote that the transition between laminar and turbulent flow in this geometry is [9,16]:

$$Re = 2 \cdot 10^4 \tag{3}$$

Our experiments were conducted utilizing the same geometry and the same stirring conditions; the value of the Reynolds number was fixed at Re = 23592 corresponding to the turbulent regime. The Schmidt number is given by:

$$Sc = \frac{\mu}{\rho \cdot D_a} \tag{4}$$

However in the following mathematical treatment we will consider a defined surface diffusivity which will be taken as one unknown in our calculations and evaluated by numerical methods. In case we consider the solid surface free energies defined as Lifshitz-van der Vaals and polar acid base interaction [17] it is reasonable to believe that calcium ions do not diffuse at the same grade from the surfaces of different sedimentary rocks.

2.3 Determining the suitable Sherwood number for the case presented

Information about the mass transfer rate from a determinate surface can be obtained by applying concepts of dimensional analysis. We indicate with L, T, M respectively a general length, time and mass and we consider the mass transfer rate, M', from a body as a function of the size, a, the velocity of the fluid, v, a diffusivity, D, the concentration difference related to the component which dissolves, Φ, and a coefficient of mass transfer, k. This is represented as Table 3.

It is assumed here that the mass transfer rate can be expressed as the sum of products of powers of the arguments:

$$M' = const \cdot a^{\alpha} \Phi^{\beta} v^{\gamma} D^{\delta} k^{\varepsilon} \tag{5}$$

Where α, β, γ, δ, ε, are unknown exponents; the dimensions of the above variables must coincide with the mass transfer rate dimensions. In this case, we have five variables and only three fundamental dimensions, for this reason it is convenient to find a simplification to the problem. It is important to note that the mass transfer coefficient has the same dimensions of the fluid velocity, in this way it will be possible to take into consideration only one characteristic velocity. The system of equations related to the exponents will be as follows:

Table 3 A qualitative dimensional analysis for limestone dissolution

Main variables

Variable	Symbol	Dimensions, M = mass, L = length, T = time
Mass transfer rate	M'	$M\,T^{-1}$
Linear dimension of the body	a	L
Velocity of the fluid	v	$L\,T^{-1}$
Difference in concentration	Φ	$M\,L^{-3}$
Diffusivity	D	L^2T^{-1}
Mass transfer coefficient	k	$L\,T^{-1}$

$$\begin{array}{ll} \beta = 1 & \text{Condition on M} \\ -\gamma - \delta = -1 & \text{Condition on T} \\ \alpha + \gamma - 3\beta + 2\delta = 0 & \text{Condition on L} \end{array}$$

Solving with respect to δ we obtain:

$$\beta = 1; \gamma = 1 - \delta; \alpha = 2 - \delta; \tag{6}$$

in this way Eq. (5) becomes:

$$M' = const \cdot \Phi \cdot a^2 \cdot v \cdot \left(\frac{D}{a \cdot v}\right)^{\delta} = \Phi \cdot a^2 \cdot v \cdot f\left(\frac{D}{a \cdot v}\right) \tag{7}$$

In the above equation, f indicates a particular function for the characteristic velocity, the mass transfer coefficient, and the diffusivity. This result gives information about the functional relation between mass transfer rate and the other variables, it can be noticed that the mass transfer rate has to be proportional to a difference in concentration, to the surface of the body considered, directly proportional to a velocity and a function of a dimensionless term. In case we consider the mass transfer coefficient as the characteristic velocity, the term in parenthesis becomes just the definition of the Sherwood number. In this way, the utilization of a function for the Sherwood number that best suits our experimental data will be justified. Previous studies have shown that limestone reacts following a first order kinetics when considering low *pH* regimes [18]. The mass transfer for a spherical particle in non-turbulent regime for high Schmidt number can be derived analytically and it is obtained utilizing the Chilton-Colburn analogy between heat and mass transfer and combining the continuity with energy balance equations. The mass transfer rate is described by [19]:

$$\dot{m} = \left(\pi d_p^2\right)(C_i - C_\infty)\left(\frac{\langle k_c \rangle}{d_p}\right)\left[\frac{(3\pi)^{\frac{2}{3}}}{2^{\frac{7}{2}}\Gamma'\left(\frac{4}{3}\right)}\right](ReSc)^{\frac{1}{3}} \tag{8}$$

the term $\left[\frac{(3\pi)^{\frac{2}{3}}}{2^{\frac{7}{2}}\Gamma'\left(\frac{4}{3}\right)}\right]$ is considered as approximately 0.991 [19]. In Eq. (8) Γ' is the so called gamma function. In our case the Sherwood number is by definition:

$$\langle k_c \rangle = Sh\left(\frac{D}{d_p}\right) \tag{9}$$

and d_p is the diameter of one single particle that has the total reaction surface. Nevertheless from Eqs. (8), (9) the Sherwood number is derived as a function of the Reynolds and Schmidt numbers:

$$Sh = \left[\frac{(3\pi)^{\frac{2}{3}}}{2^{\frac{7}{2}}\Gamma'\left(\frac{4}{3}\right)}\right](ReSc)^{\frac{1}{3}} \tag{10}$$

In literature more accurate Sherwood numbers evaluated for different Schmidt numbers are available; in our case, experimental results are well in accordance with the following empirical expression [20].

$$Sh = 2 + \left(0.4Re^{0.5} + 0.06Re^{\frac{2}{3}}\right) \cdot Sc^{0.4} \left(\frac{\mu_\infty}{\mu_w}\right)^{0.25} \tag{11}$$

The previous equation is valid for:

$$0.35 < Re < 8 * 10^4 \tag{12}$$

$$0.7 < Sc < 380 \tag{13}$$

The liquid viscosity is considered the same trough the medium, in this way the term:

$$\left(\frac{\mu_\infty}{\mu_w}\right)^{0.25} = 1 \tag{14}$$

We consider that for the sample in diluted solution of acids in water, the Schmidt number has been in the above mentioned range.

2.4 Determining the time of exposure for a determinate reacting solid surface

In the following discussion we will consider the dissolution of limestone (see Table 2) as the limiting step for the production of the required Ca^{++} ions needed to precipitate gypsum, for this reason the surface renewal theory applied to solid particles well fits our modeling purposes. When a solid sample is dissolving in turbulent flow, its surface is continuously exposed to new surfaces of fluid, while the old ones are soon mixed with the bulk. We assume that the separation layer between two phases is considered to be a sum of differential volumes and in this case we assume that each of these volumes is present for a determinate amount of time before dissolution into the bulk solution [21]. This means that each of those volumes have a different age or lifetime at the surface. The penetration theory was first announced by Higbie in the 1935 [22]: the profile of the velocity is considered to be linear at the solid–liquid interface. Accordingly the mass flux is described by the following:

$$\langle N_i \rangle = \frac{1}{L} \int_0^L \sqrt{\frac{D v_i}{\pi x}} \Delta C dx \tag{15}$$

Where N_i is the number of moles (or mass) of component i that flow through an unit of area per time, where the unit of area is fixed in the space, v_i is a characteristic interface velocity and L is the length of integration along the x axis, ΔC is the concentration difference of the component which dissolves. The quantity $\frac{L}{v_i}$ represents a time t over the integration length. Defining a surface age distribution as follows:

$\varphi(t)dt$ = fraction of particles that have an age between t and $t + dt$;

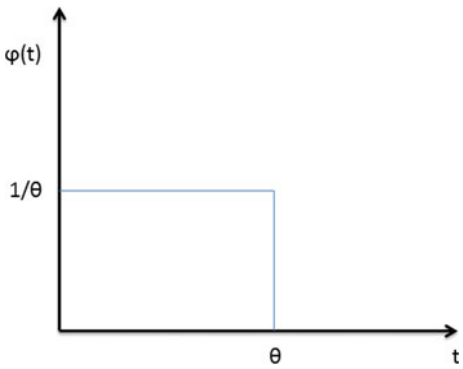

Fig. 2 φ versus θ, the case of maximum order

As a consequence:

$$\int_0^\infty \varphi(t)dt = 1 \tag{16}$$

And the average mass flux over the reaction surface is:

$$\langle \mathrm{N_a} \rangle = \int_0^\infty \Delta \mathrm{C_a} \sqrt{\frac{\mathrm{D}}{\pi t}}\, \varphi(\mathrm{t})\mathrm{dt} \tag{17}$$

where $\Delta C_a \sqrt{\frac{D}{\pi t}}$ is the mass flux for a part of surface having an age t; and $\varphi(t)dt$ represents the fraction of reaction surface that has the same age. A conceptual representation of the distribution function $\varphi\,(t)$ in case of maximum order is represented in Fig. 2.

With the assumptions made above the mass flux of the considered dissolving component is then:

$$\langle N_a \rangle = \int_0^\infty \Delta C_a \sqrt{\frac{D}{\pi t}} \varphi\,(t)\,dt = \int_0^\theta \frac{\Delta C_a}{\theta} \sqrt{\frac{D}{\pi t}} dt = 2\Delta C_a \sqrt{\frac{D}{\pi \theta}} \tag{18}$$

The mean mass transfer coefficient is obtained as:

$$\langle k \rangle = 2\sqrt{\frac{D}{\pi \theta}} \tag{19}$$

Generally the average life age and the thickness of the surface film are unknown. Here we assume a linear profile of the velocity at the interface. Equation (19) can be justified also from the following discussion: we consider a system which can be described by Fig. 3.

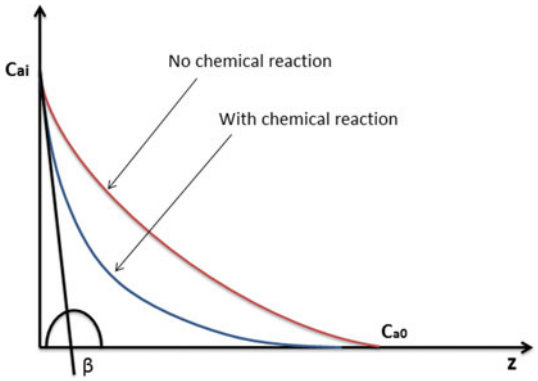

Fig. 3 Interface thickness at initial time

We indicate with δ the thickness of penetration along the Z axis given by the tangent to the curve describing the concentration profile of the component A. The molar flux at $z = 0$ is:

$$N\,(Z=0) = -D\frac{\partial C}{\partial Z}\,at\;Z=0 \rightarrow \frac{\partial C}{\partial Z} = \frac{-(C_i - C_0)}{\sqrt{\pi\,Dt}} \tag{20}$$

The Eq. (20) is a straight consequence of the following passages, in case we consider:

$$k_c\,(C_i - C_0) = -D\frac{\partial C}{\partial z} \tag{21}$$

The slope of straight line tangent at Z = 0 is:

$$\tan\beta = \frac{(C_i - C_0)}{\delta} \tag{22}$$

and for this reason:

$$\delta = \sqrt{\pi\,Dt}; \tag{23}$$

solving the integral:

$$n = \int_0^t N(t)dt = (C_i - C_0)\sqrt{\frac{D}{\pi}}\int_0^t t^{-0.5}dt = (C_i - C_0)\sqrt{\frac{D}{\pi}}2t^{-1/2} \tag{24}$$

the mean value of the mass transfer coefficient is again Eq. (19):

$$\langle k\rangle = 2\sqrt{\frac{D}{\pi t}}\quad . \tag{25}$$

Additionally it is also possible to derive the same result simplifying with assumptions the analytical solution of the differential mass balance for first order chemical reaction.

In our case for instance reactions shown in Table 2 are considered as an overall reaction of the first order [1]. This treatment however considers a different system, which is the reaction of carbon trioxide with hydronium ions, for this reason the related equations will be in a different form. The dissolution of CO_3^{2-} followed by reaction can be described by the following correlation:

$$D_A \frac{\vartheta^2[A]}{\vartheta x^2} = \frac{\vartheta[A]}{\vartheta t} + \left(k_{mn}[B_0]^n\right)[A]^m \tag{26}$$

where $[A]$ is the carbon trioxide concentration, D_A represents the diffusivity of CO_3^{2-}, x is a coordinate, B_0 is the initial hydronium ions concentration, n and m are the order of reaction with respect to the reagents hydronium and carbonic ions respectively. Equation (26) can also be obtained from a mass balance performed in spherical coordinates [12]. Equation (26) represents an accurate description of the mass transfer and reaction phenomena involved and takes into consideration the reactant other than the absorbing component; when the concentration of hydronium ions can be considered much higher than the concentration of the carbonate ions at all times, then the term $k_{mn}(B_0)^n$ would be considered as k_1, the reaction rate constant for the first order. The boundary conditions for Eq. (26) are:

$$[A] = 0, \quad if\, x \to \infty\, and\, t > 0,\ if\, t = 0\, and\, x > 0$$
$$[A] = [A^*], \quad if\, x = 0\, and\, t > 0$$

The CO_3^{2-}transfer rate expressed as an average, is obtained as follows:

$$R_A = \frac{1}{t_E}\int_0^{t_E} R_A(t)dt. \tag{27}$$

It is possible to solve analytically the partial differential equation, Eq. (26), in case m and n are equal to one, this situation is the one encountered in the case presented [23]:

$$R_A = [A^*]\left\{\sqrt{\frac{D_A}{k_1}}\left(k_1 + \frac{1}{2t_E}\right) erf\left(\sqrt{k_1 t_E}\right) + \sqrt{\frac{D_A}{\pi t_E}} exp\left(-k_1 t_E\right)\right\} \tag{28}$$

in the above equation t_E is the TOE. k_1 represents the first order reaction rate constant. By considering $k_1 t_E < 1$ Eq. (28) can be simplified as follows [24]:

$$R_A \cong [A^*] \cdot 2\sqrt{\frac{D_A}{\pi t_E}}\left(1 + \frac{k_1 t_E}{3}\right) \tag{29}$$

In case $k_1 t_E$ is far less then unity:

$$R_A \cong [A^*] \cdot 2\sqrt{\frac{D_A}{\pi t_E}} = k_L[A^*] \tag{30}$$

Last result was also obtained by Astarita in 1967 [25], in that work Astarita solved Eq. (26) by means of a Laplace transformed concentration and pointed out the possibility to utilize Eq. (30) for directly evaluating the mass transfer coefficient knowing the TOE. The model presented in Eq. (26) is valid when diffusivity phenomena take place and are limiting phenomena in the dissolution process. In case we have small particles of calcium carbonate dissolving in a BSTR where the conditions are such that the minimum stirring velocity is set for complete suspension of all the particles; the equation modeling the reaction rate can be written as:

$$\frac{dC_a}{dt} = -r + \frac{\langle k_c \rangle \cdot S}{V} \cdot (C_{ai} - C_a) \tag{31}$$

where C_a is the concentration of the carbonate ions (mol/m^3), V, the volume of the reactor, S is the reaction surface and k_c is the mass transfer coefficient (m/s). The reaction rate, r, is proportional to the concentration of the absorbing component, C_a, and to a constant, k_r, which is the reaction rate constant. In literature the second term of Eq. (31) is omitted when for instance the dissolution rate is controlled by bulk diffusion instead of surface chemical reaction, however this assumption is quite important and conditions have to be evaluated carefully [26]. For carbonate rocks with high content in calcite, Eq. (31), is confirmed with experimental data for first and second order reaction [18]. The solutions for first and second order are respectively as:

$$C_a^* = -\frac{\left(-1 + e^{(-k_r - 1/\tau)t}\right)}{\tau\,(k_r + 1/\tau)} \tag{32}$$

and

$$C_a^* = \frac{-B + \sqrt{B}\sqrt{4k_r + B}\,Tanh\left[\frac{1}{2}\left(\sqrt{B}\sqrt{4k_r + B}\,t + 2\,ArcTanh\left[\frac{\sqrt{B}}{\sqrt{4k_r + B}}\right]\right)\right]}{2k_r}; \tag{33}$$

C_a^*, is a non-dimensional concentration, $\tau = V/(\langle k_c \rangle \cdot S)$, B is equal to $1/\tau$. For the case of quasi –stationary theory and intermediate or semi-slow reaction regime, solutions given by Eqs. (32) and (33) well fit data for limestone and dolomite, however in some cases higher orders allow for a better match. Experimental data obtained for carbonate ions concentration are well in agreement with a third order chemical reaction in case of not really reactive dolomite. In the last case the mass balance expressed for a non-dimensional concentration of carbonate ions can be expressed as follows:

$$\frac{dC_a^*}{dt} = -k_r (C_a^*)^3 + \frac{\langle k_c \rangle S}{V}(1 - C_a^*) \tag{34}$$

Equation (34) can be utilized to find the best fit of experimental data for the parameters k_r and k_c with a least square numerical method by using computational methods, however the computational time required is quite large; for instance, in case we apply Eq. (34) to fit data obtained by a stepwise titration method which counts on 10 titration

steps and for which the parameters k_r and k_c have to be evaluated, then the time required is 22 min on a Intel® Core™i7 processor which is quite faster compared to lower versions. A analytical solution for Eq. (34) is given as follows: in order to simplify Eq. (34) we write: $C_a^* = Y$; $k_r = A$; and $\frac{\langle k_c \rangle S}{V} = B$ then Eq. (34) becomes:

$$\frac{dY}{dt} = -AY^3 + B(1 - Y) \tag{35}$$

the differential equation needs only one boundary condition for the concentration and the time:

$$for\, t = 0, Y = 0;$$

and the solution will be:

$$\int_0^Y \frac{dY}{-AY^3 + B(1 - Y)} = \int_0^t dt; \tag{36}$$

the left hand side of Eq. (36) requires some steps to be solved, first the substitution is applied:

$$Y^2 = P \rightarrow Y = P^{1/2} \rightarrow dy = \frac{1}{2} P^{-1/2} dP$$

leading to:

$$\int_0^Y \frac{dY}{-AY^3+B(1-Y)} = -\frac{1}{2}\int_0^Y \frac{dp}{P(AP+B)-B} = -\frac{1}{2}\int_0^Y \frac{dp}{AP^2+BP-B} \tag{37}$$

there are two zeros for $AP^2 + BP - B$ therefore:

$$P_{1,2} = \frac{-B \pm \sqrt{B^2 + 4AB}}{2A}; \tag{38}$$

giving:

$$-\frac{1}{2}\int_0^Y \frac{dp}{AP^2+BP-B} = -\frac{1}{2}\int_0^Y \frac{dp}{\left(P-\left[\frac{-B+\sqrt{B^2+4AB}}{2A}\right]\right)\left(P-\left[\frac{-B-\sqrt{B^2+4AB}}{2A}\right]\right)} \tag{39}$$

the solution for the integral on the left hand side of Eq. (36) becomes:

$$-\frac{1}{2}\int_0^Y \frac{dp}{\left(P-\left[\frac{-B+\sqrt{B^2+4AB}}{2A}\right]\right)\left(P-\left[\frac{-B-\sqrt{B^2+4AB}}{2A}\right]\right)} = \frac{-k_r}{2\sqrt{\left(\frac{k_c S}{V}\right)^2+4k_r\left(\frac{k_c S}{V}\right)}}\left\{ln\left[\frac{2k_r\cdot\left(C_a^*\right)^2+\frac{k_c S}{V}-\sqrt{\left(\frac{k_c\cdot S}{V}\right)^2+4k_r\left(\frac{k_c S}{V}\right)}}{2k_r\cdot\left(C_a^*\right)^2+\frac{k_c S}{V}+\sqrt{\left(\frac{k_c\cdot S}{V}\right)^2+4k_r\left(\frac{k_c S}{V}\right)}}\right]\right\}\Bigg|_0^{C_a^*} = t \tag{40}$$

If Eq. (40) is used instead of a numerical least square method, the computational time is reduced by several times depending on the number of data to be imported.

2.5 Empirical models

Additionally to analytical methods utilized to describe the dissolution of carbonates with acids, there are also a variety of empirical methods. In the present study, one case in particular will be discussed. Calderbank [27] gave a very useful correlation between the mass transfer coefficient between fluid and solid particles, mixed vessels were taken into account. The solid particles were considered as a single "submerged body". In the system described above the gravity force does not influence the particles motion significantly and the mass transfer is mainly influenced by the turbulence. Furthermore the model proposed by Calderbank et al. considers the mass transfer coefficient as increasing directly with the dissipated power. The correlated equation can be written as:

$$k_L\left(\frac{v_c}{D}\right)^{\frac{2}{3}} = 0.13\left(\frac{\varepsilon\mu_c}{\rho_c^2}\right)^{\frac{1}{4}} \tag{41}$$

where ρ_c is the continuous phase density (kg/m^3) and ε is the dissipated power which is given by the stirrer per unit volume of the continuous phase (W/m^3); v_c is the kinematic viscosity (m^2/sec), μ_c is the bulk viscosity (kg/(m.s)); D is the diffusion coefficient in the continuous phase (m^2/sec) and k_L is the mass transfer coefficient (m/sec). By combining Eq. (41) with a defined steady-state mass-transfer balance:

$$\frac{dV_p}{dt} = \frac{-\pi d_p^2 k_L}{\rho_m}\cdot C_h \tag{42}$$

where V_p is the volume of the limestone particle (m^3), C_h is the concentration of hydronium ions in (mol/m^3), ρ_m is the molar density (mol/m^3). Considering the dissolution of limestone in BSTR in presence of strong acid, as a sum of the dissolution rate in a stagnant system and the dissolution rate in agitated system and the Sherwood

number for free falling bodies:

$$\frac{k_L d_p}{D} = 2 \tag{43}$$

also with Eq. (42), the following equation is obtained:

$$\frac{dV_p}{dt} = -\pi \frac{C_h}{\rho_m} \cdot 2Dd_p \tag{44}$$

Combining Eq. (42) with Eq. (41) and then summing with Eq. (44) it is possible to obtain the following expression which is diverse to the one given by Toprac and Rochelle [1] because of the presence of μ_c under the term $\left(\frac{\varepsilon \mu_c}{\rho_c^2}\right)^{\frac{1}{4}}$ instead of the kinematic viscosity. The dynamic viscosity has dimensions which are in agreement with the equation presented:

$$\frac{dV_p}{dt} = -K \frac{\pi C_h}{\rho_m} \left[2Dd_p + 0.13 \left(\frac{\varepsilon \mu_c}{\rho_c^2}\right)^{\frac{1}{4}} \left(\frac{v_c}{D}\right)^{\frac{-2}{3}} d_p^2 \right] \tag{45}$$

where K is a constant of proportionality and it is dimensionless. Equation (45) can be solved analytically as follows:

By considering:

$$d_p = \left(\frac{6}{\pi}\right)^{\frac{1}{3}} V_p^{\frac{1}{3}} \tag{46}$$

With the substitutions:

$$A = -K \frac{\pi C_h}{\rho_m} 2D \left(\frac{6}{\pi}\right)^{\frac{1}{3}} \tag{47}$$

And:

$$B = -K \frac{\pi C_h}{\rho_m} 0.13 \left(\frac{\varepsilon \mu_c}{\rho_c^2}\right)^{\frac{1}{4}} \left(\frac{v_c}{D}\right)^{\frac{-2}{3}} \left(\frac{6}{\pi}\right)^{\frac{2}{3}} \tag{48}$$

The variation rate of the particle volume is then:

$$\frac{dV_p}{dt} = AV_p^{\frac{1}{3}} + BV_p^{\frac{2}{3}} \tag{49}$$

by utilizing the theorem of change of variable for continuous functions we substitute

$$V_p^{\frac{1}{3}} = G \rightarrow V_p = G^3 \rightarrow dV_p = 3G^2 dG \tag{50}$$

In the following resolution the properties of the integrals are taken into consideration. In this way the starting Eq. (49) simplifies as:

$$\frac{3G^2}{AG+BG^2}dG = dt \rightarrow \frac{3G}{A+BG}dG = dt \rightarrow \frac{3}{A}\left(\frac{G}{1+\frac{B}{A}G}\right)dG = dt \tag{51}$$

Consider $B/A = M$ after some manipulations the following expression is obtained:

$$\frac{3}{AM}\left(1-\frac{M}{M(1+MG)}\right)dG = dt \tag{52}$$

Integrating we obtain:

$$\frac{3}{AM}\left[G-\frac{1}{M}\ln(1+MG)\right]+Const. = t \tag{53}$$

When the time is t = 0, the volume $Vp = V_{p0}$ (initial condition) in this way it is possible to calculate the mentioned constant:

$$Const. = t_0 - \frac{3}{AM}\left[V_{p0}^{\frac{1}{3}} - \frac{1}{M}ln\left(1+MV_{p0}^{\frac{1}{3}}\right)\right] \tag{54}$$

Substituting the constant into the previous equation:

$$\frac{3}{AM}\left[V_p^{\frac{1}{3}} - V_{p0}^{\frac{1}{3}} + \frac{1}{M}ln\frac{\left(1+MV_{p0}^{\frac{1}{3}}\right)}{\left(1+MV_p^{\frac{1}{3}}\right)}\right] = t - t_0 \tag{55}$$

where t indicates the time for the ith fraction to change from V_{p0} to V_p.

The particle's size distribution is then taken into consideration:

$$n_{particles,i} = \frac{\Delta F_i \cdot m_{tot}}{\frac{\pi}{6}d_i^3\rho_p} \tag{56}$$

where ΔF_i is the particle's size distribution related to the ith particle class. The absolute surface of the i-class particles, $S_{tot,I}$ is obtained as follows

$$S_{tot,i} = \frac{6\Delta F_i \cdot m_{tot}}{d_i\rho_p} = n_p s_{p,i} \tag{57}$$

where $s_{p,i}$ is the surface related to one particle of the i-class and n_p is the number of particles of the i-class. In this way it is possible to obtain our V_p as a combination of the size distribution:

$$V_{p,i} = \gamma\frac{\Delta F_i \cdot m_{tot,s}}{\rho_p} \tag{58}$$

where γ is the shape factor for the ith class and it is considered to be 1 for sphere particles. Substituting the previous equation in Eq. (54) the following correlation is obtained:

$$\frac{3}{A\cdot M}\left[\left(\gamma\frac{\Delta F_i\cdot m_{tot}}{\rho_p}\right)_t^{\frac{1}{3}}-\left(\gamma\frac{\Delta F_i\cdot m_{tot,s}}{\rho_p}\right)_{t_0}^{\frac{1}{3}}+\frac{1}{M}ln\frac{\left(1+M\left(\gamma\frac{\Delta F_i\cdot m_{tot,s}}{\rho_p}\right)_{t_0}^{\frac{1}{3}}\right)}{\left(1+M\left(\gamma\frac{\Delta F_i\cdot m_{tot}}{\rho_p}\right)_t^{\frac{1}{3}}\right)}\right]=t-t_0 \tag{59}$$

The dimensionless constant K is obtained from experimental results. Taking into account only the turbulent conditions and combining Eqs. (41), (42) with the help of Eq. (46), the following expression is obtained:

$$\frac{dV_p}{dt}=-\frac{\pi C_h}{\rho_m}\left(\frac{6}{\pi}\right)^{\frac{2}{3}}V_p^{\frac{2}{3}}\cdot 0.13\left(\frac{\varepsilon\mu_c}{\rho_c^2}\right)^{\frac{1}{4}}\left(\frac{v_c}{D}\right)^{-\frac{2}{3}}; \tag{60}$$

which leads to the volume-time dependency for the i-class of particles:

$$t=\frac{3}{A_1}\left[V_{p0}^{-\frac{1}{3}}-\left(\gamma\frac{\Delta F_i\cdot m_t}{\rho_{solid}}\right)^{-\frac{1}{3}}\right]; \tag{61}$$

where A_1 is:

$$A_1=-\frac{\pi C_h}{\rho_m}\left(\frac{6}{\pi}\right)^{\frac{2}{3}}\cdot 0.13\left(\frac{\varepsilon\mu_c}{\rho_c^2}\right)^{\frac{1}{4}}\left(\frac{v_c}{D}\right)^{-\frac{2}{3}}; \tag{62}$$

Equations (58) and (60) can however be utilized only when the concentration of the hydronium ions in the solid-liquid solution is constant and other models have to be accounted for transient conditions. A named dissolution rate constant k [1] which will have the same dimensions of the constant A in this manuscript has also the same dimensions of the diffusivity (m^2/sec) for this reason the term $AV_p^{\frac{1}{3}}$ in Eq. (49) has the same dimensions of the term $D\frac{d^2V}{dx^2}$ which would be obtained by applying the Fick law to a diffusing volume, furthermore the constant B, Eq. (48), has the dimensions of (m/sec) which suggests an analogy with a volume transfer coefficient defined for this particular case; for these reasons Eq. (45) is confirmed to take into account stagnant conditions and the mass transfer rate due to agitation.

2.6 Procedure for the case study considered

The mathematical treatment and our calculations take into consideration assumptions derived from the following reasoning: due to the medium surface tension, not all the surface of the samples is in contact with the liquid phase, this suggests to consider a

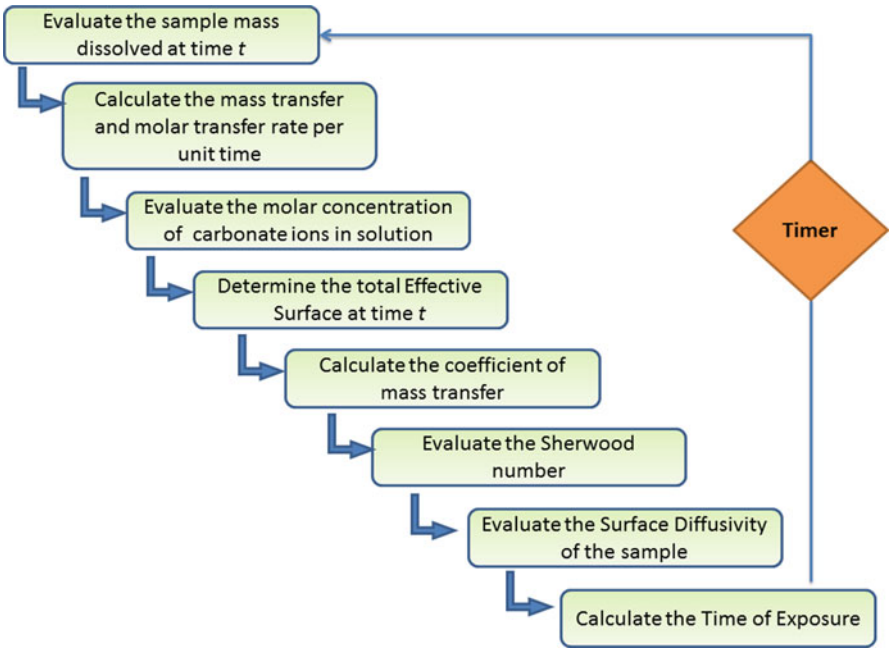

Fig. 4 Calculation procedure for evaluation the time of exposure of the sedimentary rocks

spherical layer of liquid around the particles. Taking this into account, we define an "Effective Surface" which is calculated from the PSD given by laser diffractometry; then the mass flux will be considered from the total Effective Surface. This is justified by taking into account the surface free energy of the $CaCO_3$—water system [17] and the Young-Laplace equation for the surface tension [28].

Laser diffractometry allows us to monitor on-line the PSD of our sample, for each particle size it is possible to estimate the volume, surface and number of particles. Since we refer to a surface TOE defined above, it is reasonable to refer to a related surface diffusivity, with dimensions dm^2/sec.

The surface diffusivity, the mass transfer coefficient and the TOE were evaluated by computing the experimental data obtained from *pH* measurements and laser diffractometry. From the experimental results shown in this paper it was possible to notice that for pure calcium carbonate and for non-porous surfaces (see SEM image of LJJ-01c, Fig. (6)), the surface diffusivity is well in agreement with the values obtained for Ca^{2+} ions in the same medium [29]. The calculation procedure is described in Fig. 4.

The procedure described above was performed for the totality of the measurements.

3 Materials and methods

The model: Malvern 2600 laser diffractometer was utilized for obtaining the PSD. The PSD was estimated from the distribution of the light energy which undergoes scattering. The method utilizes the theory of diffraction developed by Fraunhofer

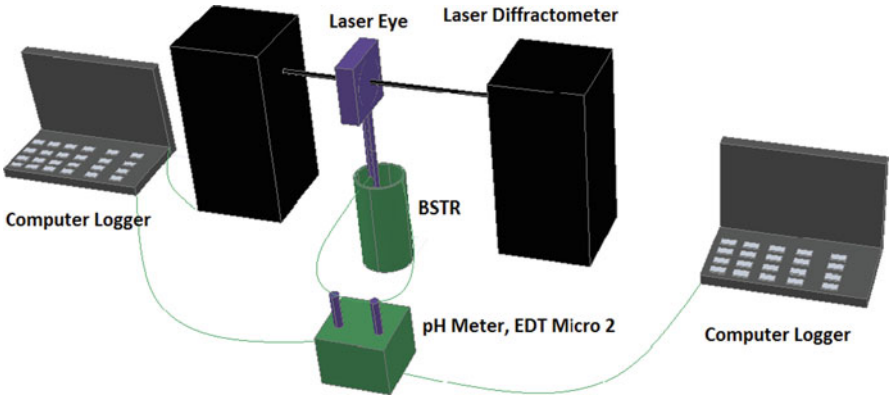

Fig. 5 Experimental equipment used for *pH* and particle size distribution measurements

[5]. One 0.5 liters batch stirred tank reactor, a laser-beam diffractometer for PSD, a *pH* electrode and a *pH* meter with temperature measurement for adjustment (EDT Micro 2) are included in the equipment. For each size range, the limestone fraction in volume was given. In this way, it has been possible to evaluate the change of the sample volume as a function of time. By laser diffractometry it was possible to verify the particle size ranges provided by the process of sieving. Additionally, the control parameters of the agitated vessel were controlled by computer loggers. The *pH* values versus *time* were estimated for each of the experiment sets. The recordings of PSD and *pH* values were synchronized. The experimental settings are described by Fig. 5.

The samples were crushed, ground and sieved to the desired particle size fractions (63–106, 106–150 and 150–250 μm), however results are demonstrated with reference to the size fraction comprises between 150 and 250 micro meters in the present study. This follows from practical reasons since with this particular particle size range it was possible to monitor the PSD in a more accurate way. The following table describes the different sedimentary rocks tested and their provenience (Table 4)

The composition of the samples tested is demonstrated in the following Table 5

The following table shows the bulk composition (as metal oxides) as weight % measured with X-ray fluorescence (XRF).

The sample indicated as Ljj-01c has Finnish origins, it is from a region called Halpanen; the sample is mostly calcite and has been described as a calcitic-carbonatite deposit in previous studies [30]. The composition of the mineral is calcite with a content of 97–99 %, additionally there is presence of apatite ($Ca_5(PO_4)_3(OH,F,Cl)$), magnesite ($MgCO_3$), pyrite (FeS_2), barite ($BaSO_4$), monazite ($(Ce, La, Th, Nd, Y)PO_4$) and fluorite. According to Puustinen and Karhu [30] the content of magnesium in the sample is low; the age was determined to be from the Paleoproterozoic period which is dated to 1,700–1,800 million years ago. Samples considered from Ljj-04c to Ljj-08c were originally provided by Tallin University of Technology in Estonia; the limestone origin was from Chinese deposits with different geological formations. Samples belong mainly to the Upper Ordovician Xiazhen, the Llandovery Hanchiatien, the Upper

Table 4 Samples tested, general classification and provenience

Sample	Description	Provenience
Ljj 01c	Paleoproterozoic magmatic limestone	Halpanen, Finland
Ljj 04c	Limestone, Llandovery Hanchiatien Fm	Daijiagou, Tongzi, Guizhou, China
Ljj 05c	Limestone, Upper Ordovician Xiazhen Fm	Zhuzhai section, Yushan, Jianxi, China
Ljj 06c	Limestone, Upper Ordovician Linshiang Fm	Wangjawan River section, Yichang, Hubei, China
Ljj 07c	Limestone, Llandovery	Daijiagou, Tongzi, Guizhou, China
Ljj 08c	Limestone, Silurian Lojoping Fm	Wulongguan section, Yichang, Hubei, China
Ljj 09c	Paleoproterozoic metamorphic limestone, marble	Parainen, Finland
TKK	Recycle materials obtained from steel converter slag used in CO_2 fixation processes	Laboratory of Energy Engineering and Environmental Protection Aalto University

Ordovician Linshang, the Silurian Lojoping and the Katian Pagoda Formations. The Hanchiatien formation is from the northern Guizhou province of China near the country town of Tongzi and the age of the sample is estimated to be from the Telychian period, 436–428.2 million years ago. In relation to the environment, the early Telychian of the upper Yangtze platform was characterized by shallow marine clastic deposits because the sea shrank and became restricted [31].

Limestone which belongs to the Lojoping formation has origins from the north of Yichang city in western Hubei Province in China. The sample is more than 400 million years old and belongs to the late Aeronian period. Samples belonging to the Linhsiang Formation are from the northeast Hunan Province in China and they are from the late Katian period, 446–456 million years ago [31]. The sample Ljj-09c is almost entirely formed by calcite, it has originated in the south-west of Finland where tectonic phenomena took place in a large area during the Precambrian period, around 1,900 million years ago. The limestone is then recrystallized as marble during the Svecofennian orogeny, seventy million years ago. The sedimentary rock was recrystallized at high temperature and pressure: 800 °C and 5 kilobars [32]. This sample shows a really regular geometry, this is demonstrated in the SEM images of Fig. 6, the regular shape of sample Ljj-09c made it possible, in previous studies, to simulate the dissolution of the sample by a modified cube root dissolution rate model [33]. Surface differences between the samples can be reasonable, this is also demonstrated in Fig. (6) where a sample belonging to the Llandovery Formation is taken into consideration (Table 3).

4 Results and discussion

During the first period of reaction, calcium carbonate is reacting effectively with H^+ ions, nevertheless when there is high concentration of carbonic acid (not strong acid), the second reaction step showed in Table 2 is slower. The experimental data related to

Table 5 Composition of the samples analyzed

Sample name Experiment number Element	(wt %)	LJJ-01C 01	LJJ-04C 01	LJJ-05C 02	LJJ-06C 03	LJJ-07C 04	LJJ-08C 05	LJJ-09C 02
CaO	%	51.8	50.1	51.7	31.1	32.1	47.9	54.5
SiO_2	%	0.38	5.2	4.6	26.6	28.7	8.0	0.50
TiO_2	%	<0.01	0.04	0.02	0.29	0.30	0.08	<0.01
Al_2O_3	%	<0.01	1.1	0.46	6.4	5.9	1.9	0.13
Fe_2O_3	%	0.66	1.0	0.24	4.6	2.4	1.1	0.16
MgO	%	0.40	0.90	0.82	1.6	1.0	0.77	0.59
K_2O	%	0.01	0.24	0.11	1.7	1.5	0.46	0.03
Na_2O	%	0.02	0.10	0.02	0.31	0.70	0.15	0.01
MnO	%	0.14	0.31	0.02	0.16	0.11	0.21	0.013
P_2O_5	%	5.1	0.06	0.01	0.04	0.06	0.04	0.006
SrO	%							
S-Eltra	%	0.13	0.02	0.03	1.5	0.02	0.03	<0.01
H.h 950°C	%	38.4	40.8	41.8	25.6	27.0	39.2	43.8
$CaCO_3$ TNV (ASTMC602)		83.0						98.5

Main compounds

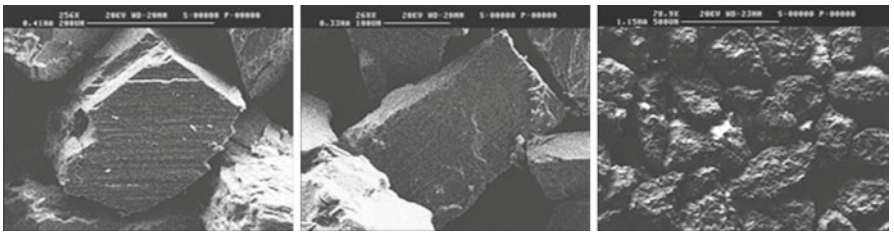

Fig. 6 Scanning electron microscope images for sample LJJ-01c (total length: 458 μm), LJJ.09c (total length: 431.6 μm) and sample Ljj. 04c (total length: 1.473 mm). Adapted from [34] with permission

the values of H^+ concentration at diverse times confirm the model presented above. The change in volume for the particles is a function of time and *pH*. Additionally the diffusion in the liquid solution has to be considered as well as the amount of sample. The titration of the solids with hydrochloric acid was performed taking into account the total mass of sample. The following table shows the experimental values related to the reaction rate of H^+ ions evaluated per unit time and per unit mass of initial sample used. It is possible to observe the different behavior of the samples. The amount of mass used was evaluated after checking the sample concentration needed for laser diffractometry, i.e. the optimal amount range of sample is a machine-dependent parameter (Table 6).

The experimental measurements for each sample given were performed during the reaction progress and the mass transfer coefficient, the total volume of solids particles;

Table 6 Hydronium ions reaction rate [mol/(sec˙grams)]

Sample Name	H^+Ions consumption [mol/(sec*grams)]
Ljj 01c	0,000323253
Ljj 04c	0,000280788
Ljj 05c	6,71497E-05
Ljj 06c	8,07072E-05
Ljj 07c	0,000153043
Ljj 08c	0,000024827
Ljj 09c	0,000212527
Tkk	1,90599E-06

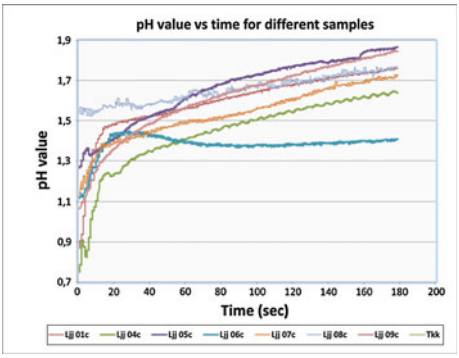

Fig. 7 Recycled materials obtained from steel converter slag used in CO_2 fixation processes

the TOE and the surface diffusivity were computed for all measurements and for each of the samples analyzed. The model considered here is developed by assuming that the change of the PSD is derived from considering particles as spheres and the distribution of the light scattering energy is evaluated by the theory of diffraction developed by Fraunhofer; the model is appropriate for opaque particles which have a radius large compared with the wavelength of the laser. The sample named as TKK in Table 4, produced at the Department of Energy Technology of Aalto University, presents particular characteristics. The sample was obtained using acetic acid to dissolve calcium from steel converter slag, then the solution containing calcium was filtered and a part of the dissolved sodium hydroxide was added to increase the *pH* level to a desired value; carbon dioxide is then bubbled through the solution at ambient pressure and thirty Celsius degrees [35]. The sample consists of various sizes of agglomerates/blocks. The following figure was obtained at the laboratories of Energy Engineering and Environ-

Table 7 Time of exposure and mean diffusivity evaluated by the model

Sample	Time of exposure (s)	Mean surface diffusivity value (dm^2/s)
Ljj 01c	1.267682333	6.60863E-06
Ljj 04c	5.323591667	1.70834E-06
Ljj 05c	3.101538333	6.72087E-06
Ljj 06c	6.058638333	1.45192E-06
Ljj 07c	16.33900333	3.7788E-07
Ljj 08c	5.621481667	7.49593E-06
Ljj 09c	0.7979	4.33001E-06
Tkk	0.276756167	8.54248E-06

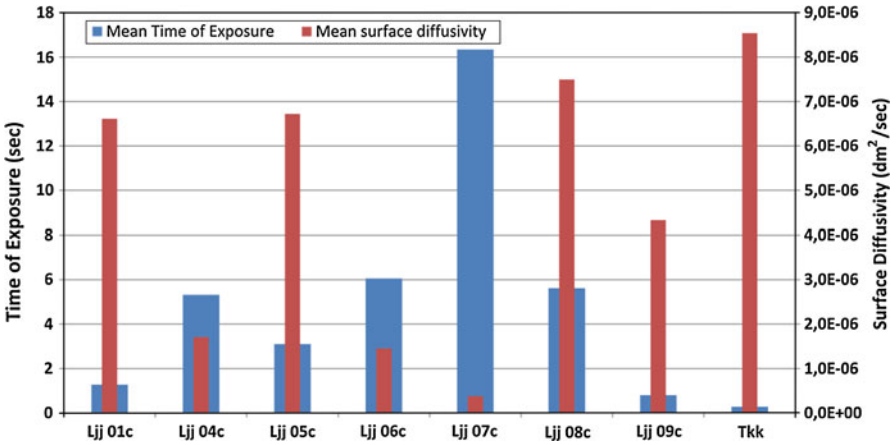

Fig. 8 Mean time of exposure and surface diffusivities for the samples analyzed

mental Protection at Aalto University; its color well describes the purity of the sample (Fig. 7; Table 7).

Here we report the results for the surface diffusivity and the TOE as mean values over the experiments (Table 7)

From the following figure a more direct comparison of the carbonates quality can be performed (Fig. 8).

The samples named as Ljj-01c, Ljj-09c and TKK are mainly constituted by pure calcium carbonate; this is reflected by the low value of TOE. As stated previously, for high purity calcium carbonate and for non-porous surfaces; the surface diffusivity is well in agreement with the diffusivity values given in literature [29]. For these samples the model was shown to be also sensitive to diverse temperatures [36] (Table 6).

5 Conclusions

A short overview on some particular mathematical models utilized for modeling sedimentary rocks dissolution in acidic environment was done with some analytical solu-

tions, one empirical model was taken into consideration and some considerations were given on their usage. The necessity to perform additional analysis on the samples utilized was brought up and in particular it was proposed that the surface tension between the bulk solution and the solid surface plays a significant role and it has to be taken into account for a proper estimation of the overall dissolution. Nevertheless quite important assumptions were present in this manuscript, for instance the solid particles where considered spherical and no solid-solid interactions were investigated.

In the present study the dissolution of sedimentary rocks and calcium carbonate obtained from CO_2 capture processes was modeled by considering the surface renewal theory. Here we consider a particular TOE for the surface including the separation layer between solid and liquid phase, from Eq. (18) we notice that the rate of dissolution will become slow after a determinate time; however in case the solid-liquid solution is stirred enough, i.e. we have turbulent conditions, the solid-liquid surface of separation is renewed in a fast way letting fresh surfaces be in contact with the particles [37]. In other words this means that the TOE will become constant for that particular Reynolds number and sample tested (Table 7).

Nevertheless this is not happening in practice, even if we consider turbulent and steady state conditions, the TOE is not exactly constant, this is because there is an avoidable presence of errors in PSD measurements, and related to the shape of the particles which in our case have been considered spherical. However the values for the TOE and the surface diffusivity are maintained nearly constant by turbulent conditions.

By using the described method it has been possible to test different qualities of carbonates in term of a TOE for reacting particles, the less the TOE the better is the quality of the sample. The method represents a tool for the evaluation and the testing of different sedimentary rocks used in FGD as well as material from CO_2 fixation processes.

Acknowledgements Academy of Finland (projects 258319 and 26495) are gratefully acknowledged for funding this work together with the Graduate School in Chemical Engineering (GSCE) at Åbo Akademi University. The Energy Engineering and Environmental Protection laboratory at Aalto University, the Process Design and Systems Engineering Laboratory and the Department of Geology at Åbo Akademi University, Finland, are highly acknowledged for providing materials and equipment. The authors acknowledge Nordkalk Corp. for the XRF measurements.

References

1. A.J. Toprac, G.T. Rochelle, Environ. Prog. Sustain. Energy **1**(1), 52 (1982)
2. L. Kasoer, H. Scott Fogler, C.C. McCune, Chem. Eng. Sci. **28**(2), 691–700 (1973)
3. D. Binlin, P. Weiguo, J.W. Qiang, Wenhuan Yu Li, Energy Convers. Manag. **50**(10), 2547–2553 (2009)
4. C. De Blasio, Claudio Carletti, Lauri Järvinen, Tapio Westerlund, Comput. Aided Chem. Eng. **29**, 1225–1229 (2011)
5. C. De Blasio, E. Mäkilä, T. Westerlund, Appl. Energy Elsevier **90**(1), 175–181 (2012)
6. Alexander Apelblat, Chem. Eng. J. **19**(1), 19–37 (1980)
7. M.H. Al-Khaldi, H.A. Nasr-El-Din, S. Mehta, A.D. Al-Aamri, Chem. Eng. Sci. **62**(21), 5880–5896 (2007)
8. Maud Gautelier, Eric H. Oelkers, Jacques Schott, Chem. Geol. **157**(1), 13–26 (1999)
9. H. Kasper Lund, Scott Fogler, Chem. Eng. Sci. **28**(3), 691–700 (1973)
10. R. Zhang, S. Hu, X. Zhang, W. Yu, Aquat. Geochem. **13**, 309–338 (2007)
11. B.B. Williams, J.L. Gidley, J.A. Guin, R.S. Schechter, Ind. Eng. Chem. Fundam. **9**(4), 589–596 (1970)
12. H.S. Carslaw, J.C. Jaeger, *Conduction of heat in solids*, 2nd edn. (Clarendon Press, Oxford, 1959)

13. C. Carletti, F. Bjondahl, C. De Blasio, J. Ahlbeck, L. Järvinen, T. Westerlund, Environ. Prog. Sust. Energy. (2012). doi:10.1002/ep.11683
14. S. Kiil, *Experimental and Theoretical Investigations of Wet Flue Gas Desulfurization* (Tekst & Tryk A/S, Vedbaek, 1998)
15. A.R. Hendrickson, R.B. Rosene, D.R. Wieland, Acid reaction parameters and reservoir characteristics used in the design of acidizing treatments. ACS Div. Petrol. Chem. **5**, 45–55 (1960)
16. S. Ibrahim, A.W. Nienow, Chem. Eng. Res. Des. **73**(5), 485–491 (1995)
17. B. Sameer, S. Dunn, B. Jefferson, V. Macadam, Appl. Surf. Sci. **255**, 4873–4879 (2009)
18. C. De Blasio, C. Carletti, K. Lundqvist, L. Saeed, T. Westerlund, C.-J. Fogelholm, Comput. Aided Chem. Eng. Els. **31**, 465–469 (2012)
19. R. Biron Bird, W.E. Stewart, E.N. Lightfoot, *Transport Phenomena* (Wiley, Singapore, 1960)
20. Ismail Tosun, *Modeling in Transport Phenomena* (Elsevier Science, Amsterdam, 2002)
21. P.V. Danckwerts, Unsteady-state diffusion or heat-conduction with moving boundary. Trans. Faraday Soc. **46**, 701–712 (1950)
22. R. Higbie, Trans. Am. Inst. Chem. Eng. **31**, 65 (1935)
23. P.V. Danckwerts, Trans. Faraday Soc. **47**, 1014–1023 (1951)
24. L.K. Doraiswamy, M.M. Sharma, *Heterogeneous Reactions Analysis Examples and Reactor Design*, vol. 2 (Wiley, USA, 1984)
25. G. Astarita, *Mass Transfer with Chemical Reaction* (Elsevier Publishing Company, Amsterdam, 1967)
26. A. Lorenzo Fusi, M.Primicerio Monti, Journal of Mathematical Chemistry. DOI (2012). doi:10.1007/s10910-012-0045-3
27. P.H. Calderbank, M.B. Moo-Young, Chem. Eng. Sci. **16**(1–2), 39 (1961)
28. P.S. de Laplace, *Mechanique Celeste, English version* (Butt Press, Isaac R, 1806)
29. P.K. Chan, G.T. Rochelle, Am. Chem. Soc. Symp. Ser. **188**, 75–97 (1982)
30. K. Puustinen, J. Karhu, Geol. Surv. Finl. **27**, 39–41 (1999)
31. J. Rong, X. Chen, Z. Zhou, Z. Wang, Y. Zhang, J. Liu, P. Chen, J. Fan, W. Juan, Y. Zhang, R. Wu, *Ordovician-Early Silurian (Llandovery) Stratigraphy and Palaeontology of the Upper Yangtze Platform, South China* (Science Press Beijing, Nanjing, 2007)
32. M. Väisänen, P. Hölttä, Bull. Geol. Soc. Finl. **71**(1), 177–218 (1999)
33. C. De Blasio, E. Mäkilä, T. Westerlund, Comput. Aided Chem. Eng. Els. **26**, 821–826 (2009)
34. C. De Blasio, *Reactive Dissolution of Sedimentary Rocks in Flue Gas Desulfurization, Modeling and Experimental Investigation* (Painosalama OY, Turku, 2010). ISBN 978-952-12-2482-9
35. S. Teir, S. Eloneva, R. Zevenhoven, Energy Conv. Manag. Els. **46**, 2954–2979 (2005)
36. C. De Blasio, J. Ahlbeck, Tapio Westerlund. Comput. Aided Chem. Eng. **27**, 411–416 (2009)
37. P.V. Danckwerts, Ind. Eng. Chem. **43**(6), 1460–1467 (1951)